Table IX. Absorption Spectra and Co–N Bond Lengths of $[Co(diamine)_3]^{3+}$ Complexes

complex[a]	λ, nm	log ε, M^{-1} cm^{-1}	av Co–N dist, Å[e]
$[Co(en)_3]^{3+}$ [b]	467	1.97	1.964 (1)[f]
	339	1.93	
	212	4.36	
$[Co(meen)_3]^{3+}$ [c]	492	2.06	
	351	2.01	
	231	4.36	
$[Co(tn)_3]^{3+}$ [b]	490	1.88	1.979 (5)[g]
	351	1.88	
	231	4.38	
$[Co(tmd)_3]^{3+}$ [b]	502.5	1.92	1.991 (5)[h]
	357	1.87	
	232	4.38	
Λ-$[Co(S,S\text{-dppn})_3]^{3+}$ [d]	506	2.06	
mer-$[Co(ama)_3]^{3+}$	514	2.14	1.998 (7)
	365	2.10	
	243	4.35	

[a] All solutions 10^{-3} M in H_2O. Abbreviations: en = 1,2-ethanediamine; meen = *N*-methyl-1,2-ethanediamine; tn = 1,3-propanediamine; tmd = 1,4-butanediamine; dppn = 1,3-diphenyl-1,3-propanediamine. [b] Reference 25. [c] Reference 23. [d] Reference 26. [e] Errors were calculated as the estimated standard deviations in the derived mean Co–N values. [f] Reference 3. [g] Reference 5. [h] Reference 4.

the chelating ligands are expected to make the dominant contribution to the expansion of the CoN_6 chromophore. Additionally, the azetidine moieties inhibit the conformational freedom of the chelate rings. Both factors could constrain the orbital orientation and overlap of the nitrogen donors and weaken the metal/donor atom interactions.

No other $[Co(diamine)_3]^{3+}$ ions with six-membered chelate rings and secondary nitrogen donors appear to have been reported, although a range of complexes $[Co(N\text{-Ren})_3]^{3+}$ (*N*-Ren = *N*-alkylethylenediamine) have been prepared.[27] The $[M(ama)_3]^{n+}$ species constitute a novel addition to the known series of $[M(diamine)_3]^{n+}$ complexes.

Acknowledgment. We are grateful to the Research School of Chemistry workshop staff and B. E. Fenning for the installation of the high-pressure autoclave, to The Australian National University Microanalytical Unit, and D. Bogsanyi for the pK_a measurements. M.G.M. is grateful to The Australian National University for a Postgraduate Research Award.

Registry No. ama·2HCl, 96308-73-5; *mer*-$[Co(ama)_3]Cl_3·3H_2O$, 96308-74-6; *cis*-$[Co(ama)_2(OH_2)(Cl)](Cl)ClO_4$, 96326-16-8; *cis*-$[Co(ama)_2(OH_2)_2]^{3+}$, 96308-75-7; $[Ni(ama)_3](ClO_4)_2$, 96326-20-4; $[Co(ama)_2(OH)(OH_2)_2](ClO_4)_2$, 96326-18-0; ethylidynetris(methylenebenzenesulfonate), 31044-85-6.

Supplementary Material Available: Fractional coordinates for hydrogen atoms (Table IIa), anisotropic thermal parameters for non-hydrogen atoms (Table IIb), interatomic distances involving hydrogen atoms within the ligand complex (Table IIIa), and a listing of observed and calculated structure factor amplitudes (15 pages). Ordering information is given on any current masthead page.

(27) Keller, R. N.; Edwards, L. J. *J. Am. Chem. Soc.* **1952**, *74*, 215.

Contribution from the Department of Chemistry, City University of New York, Queens College, Flushing, New York 11367, and Corning Glass Company, Corning, New York 14830

Reactions of $W(CO)_5$ Adsorbed onto Porous Vycor Glass with Various Ligands

ROBERT C. SIMON,[†] HARRY D. GAFNEY,*[†] and DAVID L. MORSE[‡]

Received April 24, 1984

UV photolysis of $W(CO)_6$ physisorbed onto porous Vycor glass, PVG, leads to the corresponding pentacarbonyl. Electronic and EPR spectra indicate that the latter has a square-pyramidal, C_{4v}, structure with either a silanol group or chemisorbed water occupying the vacated coordination site. Exposing the pentacarbonyl to various ligands, either as gases or in a solution of degassed *n*-hexane, leads to displacement of the PVG surface functionality and formation of adsorbed $W(CO)_5L$ or $W(CO)_4L$ when L is bidentate. The pressure dependence of the reactions with gaseous ligands suggests that, at higher pressure, the predominant mode of reaction is between $W(CO)_5$ and a mobile, coadsorbed ligand. The activation parameters of the reaction with CO, which is weakly adsorbed onto PVG, indicate that the $W(CO)_5$–PVG interaction energy is ≤7 kcal/mol.

Introduction

Photolysis of the group 6[1] hexacarbonyls physisorbed onto porous Vycor glass, PVG, yields the corresponding pentacarbonyls.[2a] UV–visible spectra of the latter, particularly the W analogue, resemble spectra of $W(CO)_5L$ species, where L is an O-donor ligand.[2b] Since hydroxylated silica supports can be viewed as polydentate ligands,[3-6] the spectral similarity suggests that the long lifetime of the adsorbate, designated $W(CO)_5$(ads), is due to coordination to PVG. Stability gained through coordination to the support is advantageous with respect to spectroscopic characterization, but breaking this bond, which may be a necessary prerequisite to further reactivity, could represent a costly, endergonic activation step.

Previous studies of the thermal activation of these complexes physisorbed onto SiO_2 or Al_2O_3 indicate that formation of surface carbonyl species is reversible, although, in general, reversibility requires elevated temperatures. Howe, for example, reports that warming the complexes on SiO_2 above 10 °C in vacuo causes IR bands characteristic of the hexacarbonyl to disappear.[8] The

[†] City University of New York.
[‡] Corning Glass Co.

(1) In this paper the periodic group notation is in accord with recent actions by IUPAC and ACS nomenclature committees. A and B notation is eliminated because of wide confusion. Groups IA and IIA become groups 1 and 2. The d-transition elements comprise groups 3 through 12, and the p-block elements comprise groups 13 through 18. (Note that the former Roman number designation is preserved in the last digit of the new numbering: e.g., III → 3 and 13.)
(2) (a) Simon, R. C.; Morse, D. L.; Gafney, H. D. *Inorg. Chem.* **1983**, *22*, 573. (b) Wrighton, M. S. *Chem. Rev.* **1974**, *74*, 401.
(3) Ahrland, S.; Grenthe, I.; Noren, B. *Acta Chem. Scand.* **1960**, *14*, 1059.
(4) Wolf, F.; Renger, P.; Janowski, F.; Heyer, W. *Z. Anorg. Allg. Chem.* **1977**, *432*, 249.
(5) Stanton, J. H.; Maatman, J. *J. Phys. Chem.*, **1964**, *68*, 757.
(6) Burwell, R. L. *CHEMTECH* **1974**, 370.
(7) Bailey, D. C.; Langer, S. H. *Chem. Rev.* **1981**, *81*, 109.
(8) Howe, R. F. *Inorg. Chem.* **1976**, *15*, 486.

0020-1669/85/1324-2565$01.50/0

reaction could be reversed, although the extent of reversibility at 45 °C depends on CO pressure and exposure time. Brenner and Burwell report that the decomposition of $Mo(CO)_6$ on Al_2O_3, which ultimately yields $Mo(CO)_3$(ads), is completely reversible at 100 °C.[9] Similar results were obtained in the thermal decomposition of $W(CO)_6$ on Al_2O_3, where ≥73% of the hexacarbonyl was regenerated on exposure to CO at 175 °C.[10]

From the chemical point of view, i.e., the functional groups on the surfaces, the reactivity of an adsorbate on PVG might be expected to resemble that found on silica gel. On the other hand, these highly irregular surfaces are fractal with substantially different fractal dimensions.[11-13] The Hausdorff or fractal dimension of PVG, 1.74 ± 0.12,[14] is unusually small.[11] Pfeifer and Avnir point out that chemical factors may be secondary to geometrical factors in influencing adsorbate reactivity on a highly irregular surface.[12] To gain some insight into the energetics of the PVG–$W(CO)_5$ interaction and the mechanism by which the adsorbate reacts on this surface, the reactions of the adsorbed pentacarbonyl, $W(CO)_5$(ads), with a series of mono- and bidentate ligands have been examined.

Spectra recorded after exposure to mono- and bidentate ligands, either as a gas or in a solution of *n*-hexane, establish quantitative formation of $W(CO)_5L$(ads) or $W(CO)_4L$(ads). The reactions of the adsorbed species are analogous to solution-phase substitution reactions except that the incoming ligand displaces the surface functionality occupying the vacated coordination site. When L is in the gas phase, the pressure dependence of the reaction rate constant suggests two modes of reaction. The activation energies of the reactions indicate that the $W(CO)_5$–PVG interaction, while sufficient to stabilize the pentacarbonyl, is relatively weak, ≤7 kcal/mol, and is not a significant barrier to further reactivity.

Experimental Section

Materials. $W(CO)_6$ was purchased from Pressure Chemical Co. and was used without further purification since UV–visible and infrared spectra of the complex were in excellent agreement with published spectra.[2b,15] $W(CO)_4$(bpy) (bpy denotes 2,2′-bipyridine) was prepared by 350-nm photolysis of N_2-purged, 25 °C, *n*-hexane solutions of $W(CO)_6$ in the presence of 1 equiv of bpy (Aldrich). The product, which precipitated from the photolyzed solution, was recrystallized from CH_2Cl_2 and its UV–visible, emission, and infrared spectra were in excellent agreement with published spectra.[2b,15,16] Other than being dried, gaseous reagents (Linde) were used without further purification since each had a purity level of ≥99%. All solvents used in these experiments were HPLC grade and were dried over molecular sieves.

Code 7930 porous Vycor glass, PVG, containing 7.0 ± 2.0 nm diameter pores was obtained from the Corning Glass Co. Pieces of PVG 25 mm × 25 mm × 4 mm were placed in a Soxhlet extractor and continuously extracted, first with acetone for 12 h and then with distilled water for the same period of time. The extracted pieces were dried under reduced pressure in a vacuum oven at 50 °C and then calcined at 650 °C either in a muffle furnace or under flowing O_2 or H_2 in a tube oven for ≥72 h. The calcined PVG samples were cooled to room temperature and stored under vacuum.

Impregnation with $W(CO)_6$ was by conventional procedures.[17] PVG samples were placed in 50 mL of a 10^{-2} M *n*-hexane solution of $W(CO)_6$ for 4–12 h, and the moles of complex adsorbed were calculated from the change in the UV spectra of the solution phase. Hexane incorporated during impregnation was removed under vacuum, $p \leq 10^{-4}$ torr, at room temperature. Diffuse-reflectance FTIR and mass spectral studies, which will be described elsewhere, confirmed removal of the solvent under these conditions. The impregnated samples used in these experiments contain from 1.24×10^{-5} to 3.09×10^{-5} mol of $W(CO)_6$ or 2.76×10^{-6} to 6.87×10^{-6} mol of complex/g of PVG. Impregnation with $W(CO)_4$(bpy) was by the same procedure except that the complex was dissolved in CH_2Cl_2 rather than hexane.

The impregnated sample was rigidly mounted with a Teflon holder in a 4 cm × 2.2 cm × 1 cm rectangular quartz or Pyrex cell and evacuated, $p \leq 10^{-4}$ torr. $W(CO)_5$(ads) was generated in situ via 350-nm photolysis in a Rayonet photochemical reactor (Southern New England Ultraviolet Corp.). UV–visible spectra were recorded during photolysis to monitor formation of the pentacarbonyl, and photodissociated CO was removed by pumping. The photochemical reaction was limited to ≤25% consumption of $W(CO)_6$ to prevent further decarbonylation of the pentacarbonyl via secondary photolysis.[2a]

Kinetics Measurements. To measure the rate of reaction between $W(CO)_5$(ads) and a gaseous ligand, the evacuated cell containing the pentacarbonyl was attached to the vacuum line, and the cell and a bulb containing a known pressure of the ligand were thermostated to the same temperature with water baths. After thermal equilibration, the gaseous ligand was expanded into the cell, the equilibrium pressure was measured, and the cell was closed off. Expansion lowers the gas temperature, but the reaction rates were slow enough to allow reequilibration to the original temperature. The charged cell was placed in a thermostated cell holder of a spectrophotometer, and spectra were recorded periodically. A shutter in the spectrophotometer prevented photolysis of the sample. The adsorption isotherms of the different ligands on PVG were measured under similar conditions according to previously described manometric procedures and corrected for adsorption onto surfaces other than PVG.[18]

Nonvolatile ligands were added as *n*-hexane solutions. The cell containing the $W(CO)_5$(ads) sample was attached to the vacuum line through a section having a side arm containing the ligand solution. The cell and enclosed PVG sample were evacuated, and the ligand solution was degassed by repeated freeze–pump–thaw cycles. After degassing, the cell and attached side arm were closed off, removed from the line, and inverted to flow the ligand solution onto the PVG sample.

Physical Measurements. Gases generated during the photogeneration of $W(CO)_5$(ads) were collected in a 4.4-mL sample loop with a Toepler pump. The sample loop was transferred to a Gow-Mac Model 100-69 gas chromatograph equipped with a 6 ft × $^1/_4$ in. i.d. stainless-steel column packed with 80–100 mesh, 5-Å molecular sieves (Supelco Corp) and a Re–W thermal conductivity detector. The detector response was calibrated with known amounts of CO (Linde) and displayed on a Shimadzu R-111 recorder. Absorption spectra were recorded on a Cary 14 or Tektron 635 spectrophotometer equipped with thermostated rectangular cell holders. Emission spectra were recorded on a Perkin-Elmer Hitachi MPF-2A emission spectrophotometer equipped with a Hamamatsu R818 red-sensitive photomultiplier. The sample arrangement within the emission spectrophotometer has been previously described.[18] EPR spectra of the complexes adsorbed onto crushed (60–80 mesh) PVG were recorded at room temperature, 22 ± 1 °C, or 77 K on an IBM-Bruker Model ER200E-SCR spectrometer. The resonance Raman spectrometer has been previously described,[19] and the spectra described in this paper were recorded by means of 90° transverse excitation with the 457.9-nm Ar laser line. Absorption spectra, recorded before and after scanning the Raman spectrum, showed that the laser excitation did not cause a detectable photochemical change.

Results

Generally, three PVG samples were impregnated simultaneously. After removal of the solvent, absorption spectra of the individual samples and spectra recorded at different locations on the same sample are within an experimental error of ≤8%, which establishes reproducible impregnation and a uniform distribution of $W(CO)_6$ on the PVG surface. The cross-sectional distribution was determined by described grinding and optical density measurements.[18] Previous experiments suggest that heat generated during impregnation by grinding a support with a metal carbonyl causes some complexes to decompose and, in the presence of air, oxidize.[20-22] However, no spectral evidence was found that grinding under the described conditions caused either decomposition or oxidation. Furthermore, with colored adsorbates, such as $W(CO)_4$(bpy), penetration depths measured by grinding were in excellent agreement with penetration depths determined by

(9) Brenner, A.; Burwell, R. L. *J. Am. Chem. Soc.* **1975**, *97*, 2565.
(10) Brenner, A.; Hucul, D. A. *J. Catal.* **1980**, *61*, 216.
(11) Avnir, D.; Farin, D., *Nature (London)* **1984**, *308*, 261.
(12) Pfeifer, P.; Avhir, D. *J. Chem. Phys.* **1983**, *79*, 3558.
(13) Avnir, D.; Farin, D.; Pfeifer, P. *J. Chem. Phys.* **1983**, *79*, 3655.
(14) Evan, U.; Rademan, K.; Jortner, J.; Manor, N.; Reisfeld, R. *Phys. Rev. Lett.* **1984**, *52*, 2164.
(15) Jones, L. H. *Spectrochim. Acta* **1963**, *19*, 329.
(16) Angelici, R. J.; Jacobson, S. E.; Ingemanson, C. M. *Inorg. Chem.* **1968**, *7*, 2466.
(17) Innes, W. B. "Catalysis"; Emmett, P. H. Ed.; Reinhold: New York, 1954; Vol. I, p 245.
(18) Wolfgang, S.; Gafney, H. D. *J. Phys. Chem.* **1983**, *87*, 5395.
(19) Valance, W. G.; Strekas, T. C. *J. Phys. Chem.* **1982**, *86*, 1804.
(20) Brenner, A.; Burwell, R. L. *J. Catal.* **1978**, *52*, 353, 364.
(21) Howe, R. F.; Kemball, C. *J. Chem. Soc., Faraday Trans. 1* **1974**, *70*, 1153.
(22) Howe, R. F.; Leith, I. R. *J. Chem. Soc., Faraday Trans.* **1973**, *69*, 1967.

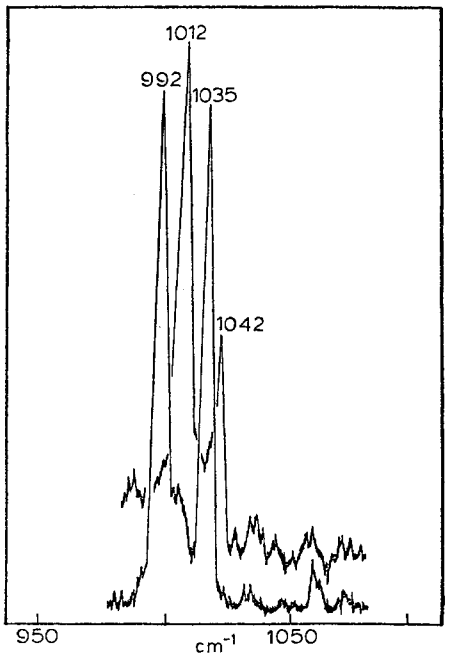

Figure 1. Raman spectrum of pyridine adsorbed onto PVG and resonance Raman spectrum of $W(CO)_5(py)(ads)$ generated in situ.

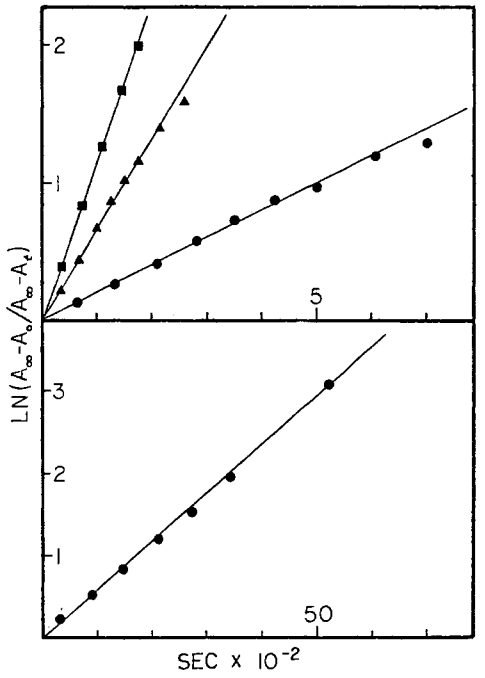

Figure 2. First-order plots of the reactions of $W(CO)_5(ads)$. Top: with CO (●); with *cis*-2-butene (▲); with *trans*-2-butene (■). Bottom: with 2,2′-bipyridine.

breaking the sample in half and measuring the depth of color under a microscope. Penetration depth is controlled principally by exposure times longer than the 4–12 h used in these experiments.

As previously described, the electronic and vibrational spectra of $W(CO)_6(ads)$ closely resemble those of the complex in fluid solution.[1] Photolysis of $W(CO)_6(ads)$ evolves 1.0 ± 0.1 mol of CO/mol of complex reacted and yields an adsorbed photoproduct with an optical spectrum equivalent to that of $W(CO)_5$ in 20 K CH_4 matrix.[23] The low-energy absorption of the photoproduct, 410 nm, is similar to the $^1A \rightarrow {}^1E$ transition maxima of $W(CO)_5(CH_3COCH_3)$ and $W(CO)_5((CH_3CH_2)_2O)$, 406 and 418 nm, respectively.[24] This spectral similarity and the absence of an ESR signal suggest that $W(CO)_5(ads)$ is of C_{4v} symmetry with either a silanol group or chemisorbed water occupying the vacated coordination site. Thus, stability of $W(CO)_5(ads)$ appears to arise from coordination to PVG, but this does not curtail subsequent thermal reactivity.

The photoreaction is readily reversed at room temperature, 22 ± 1 °C, by exposure to CO. Exposure causes a decline in absorbance at 410 nm and a concurrent increase in absorbance at 289 nm, characteristic of the original hexacarbonyl. The amount of $W(CO)_6(ads)$ regenerated in the reaction, however, depends on the extent of photolysis of the original hexacarbonyl. Provided the isosbestic point is maintained during photolysis, i.e., the photoreaction is limited to ≤40% consumption of $W(CO)_6(ads)$, the thermal back-reaction under 1 atm of CO regenerates ≥97% of the original hexacarbonyl. Loss of the isosbestic point implies secondary photoreaction(s) that reduce quantitative reversibility.

Thermal reactivity occurs with a variety of ligands. Exposing a 22 ± 1 °C PVG sample containing 1.24×10^{-5} mol of $W(CO)_5(ads)$ to 15 torr of gaseous pyridine causes the 410-nm band to disappear and be replaced by a band at 390 nm. The latter is in excellent agreement with the reported solution spectrum of $W(CO)_5(py)$.[24] Excitation of the adsorbed reaction product at room temperature with 390-nm light induces an emission centered at 526 nm, which also agrees with the reported 524-nm emission maximum of $W(CO)_5(py)$ in a 77 K methylcyclohexane glass.[25] As illustrated by Figure 1, pyridine adsorbed onto PVG exhibits two intense symmetric vibrations at 992 and 1035 cm^{-1} whereas that adsorbed onto PVG containing $W(CO)_5(ads)$ exhibits bands at 1012 and 1042 cm^{-1}. The wavelength dependence of the vibrational intensity indicates that the former spectrum is a preresonance spectrum whereas the latter is a resonance Raman spectrum. Since the resonance condition requires excitation incident with electronic absorption of the molecule, the occurrence of pyridine vibrations in the spectrum as well as their change in relative intensities and shifts to higher wavenumbers[26] establishes py coordination and formation of $W(CO)_5(py)(ads)$.

Exposure to *cis*- or *trans*-2-butene, 1,3-butadiene, 1-butene, or 1-pentene causes spectral changes indicative of alkene coordination to the pentacarbonyl. In each reaction, the 410-nm band characteristic of $W(CO)_5$ disappears and a new absorption band appears in the 300–305-nm region as a shoulder on the more intense UV absorptions along with a weaker band in the 350–360-nm

Table I. Parameters for the Reaction $W(CO)_5(ads) + L$

ligand L	temp, K	mol of L adsorbed × 10^5	mol of $W(CO)_5(ads)$ × 10^6	$10^3 k_{expt}$, s^{-1}	E_a, kcal/mol
CO	275	2.58	2.20	1.01	6.97
	305	2.58	1.51	3.48	
	325	2.30	1.24	6.33	
	350	2.15	1.82	12.7	
cis-2-butene	275	1.22	2.54	0.299	20.39
	305	0.599	2.41	5.85	
	325	0.579	2.41	46.0	
	350	0.583	2.06	442.0	
trans-2-butene	275	1.15	2.13	2.46	6.05
	305	1.16	3.09	7.32	
	325	1.12	2.41	13.2	
	350	1.11	2.34	24.8	
1-pentene[a]	275		2.30	0.0912	16.68
	305		2.41	2.04	
	325		2.82	11.2	
	350		2.61	70.8	
2,2′-bipyridine[b]	275		3.15	0.55	

[a] Added as a degassed, neat liquid. [b] Added as a degassed 10^{-2} M *n*-hexane solution.

(23) Perutz, R. N.; Turner, J. J. *J. Am. Chem. Soc.* **1975**, *97*, 4791.
(24) Wrighton, M. S.; Hammond, G. S.; Gray, H. B. *Inorg. Chem.* **1972**, *11*, 3122; *J. Am. Chem. Soc.* **1971**, *93*, 4336.
(25) Wrighton, M. S.; Abrahamson, H. B.; Morse, D. L. *J. Am. Chem. Soc.* **1976**, *98*, 4105.
(26) Zingaro, R. A.; Witmer, W. B. *J. Phys. Chem.* **1960**, *64*, 1705.

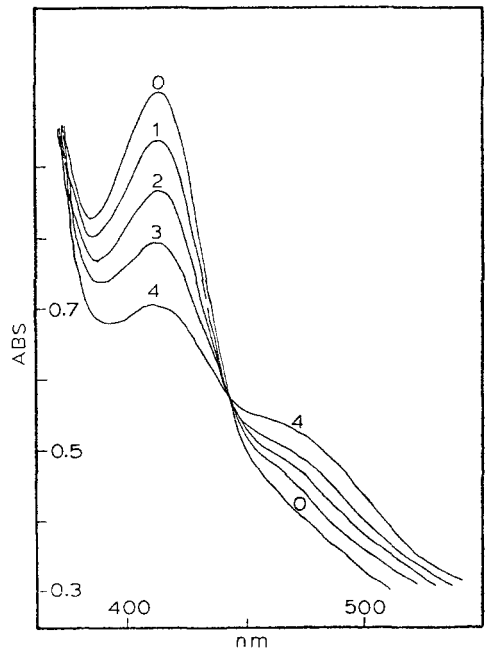

Figure 3. Spectral changes following exposure of 1.2×10^{-6} mol of $W(CO)_5$(ads) to a 10^{-2} M hexane solution of 2,2′-bipyridine.

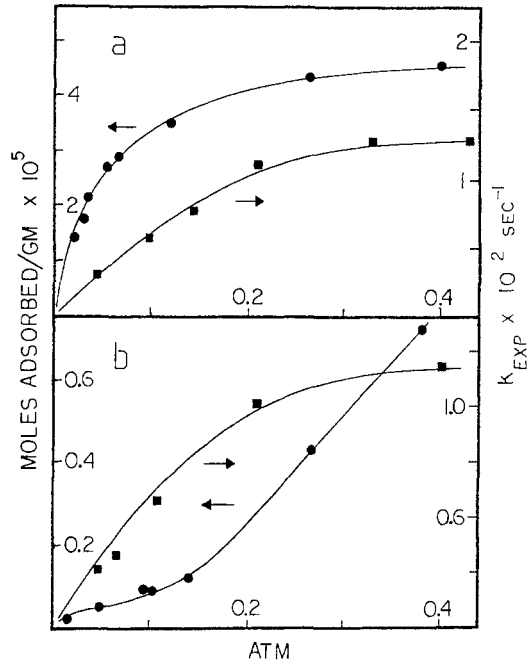

Figure 4. (a) Adsorption isotherm of CO on PVG (●) and the dependence of the rate constant for its reaction with $W(CO)_5$(ads) on the CO pressure (■). (b) Adsorption isotherm of *cis*-2-butene on PVG (●) and the dependence of the rate constant for its reaction with $W(CO)_5$(ads) on the *cis*-2-butene pressure (■).

region. The 1-pentene–$W(CO)_5$(ads) product spectrum agrees with the reported spectrum of $W(CO)_5$(1-pentene),[27] and the amount of product formed, calculated on the assumption that the ratio of the extinction coefficients of adsorbed $W(CO)_6$ and $W(CO)_5$(1-pentene) is equivalent to that found in fluid solution, differs by ≤3% from the amount of $W(CO)_5$ generated during photolysis. The stoichiometric agreement indicates that, at least during these reaction times, the alkenes react exclusively with $W(CO)_5$(ads).

In the presence of excess ligand, the thermal reactions follow pseudo-first-order kinetics, as illustrated in Figure 2, through 3–4 half-lives, although deviations do occur beyond this point. The rate constants calculated from the slope of these plots, k_{expt}, are listed in Table I. The activation parameters for the different reactions were determined at a given ligand pressure over the temperature range of 275–340 K. The Arrehenius plots are linear, and the activation parameters calculated from these plots are listed in Table I.

As shown in Figure 3, exposing a PVG sample containing 1.2×10^{-6} mol of $W(CO)_5$(ads) to a degassed 1.0×10^{-2} M *n*-hexane solution of 2,2′-bipyridine causes a decline in absorbance at 410 nm and a concurrent growth in absorbance at 490 nm. The product spectrum agrees with the solution spectrum of $W(CO)_4$(bpy) and with the spectrum of $W(CO)_4$(bpy) adsorbed onto PVG. Excitation of the adsorbed reaction product with 490-nm light induces an emission with a maximum at 683 nm, which also agrees with the 680-nm emission maximum reported for 298 K solid samples of $W(CO)_4$(bpy).[24] The spectral data establish the reaction product to be $W(CO)_4$(bpy), and the amount formed, calculated by means of an effective extinction coefficient obtained from the spectrum of a PVG sample containing adsorbed $W(CO)_4$(bpy), indicates that bpy reacts only with $W(CO)_5$(ads). Throughout the reaction, an isosbestic point is maintained at 440 nm, and although the reaction involves displacement of a second CO ligand, there is no spectral evidence of a long-lived, monodentate bpy intermediate. As shown in Figure 4, the spectral changes conform to a pseudo-first-order reaction with a rate constant of $(5.5 \pm 0.4) \times 10^{-4}$ s^{-1}.

The impregnated samples used in these experiments initially contain ≤3.09×10^{-5} mol of $W(CO)_6$, which uniformly impregnates a volume of PVG equal to the product of the geometric surface area and the penetration depth, 0.3–0.4 nm. In a fractal with an unusually small fractal dimension,[11-14] i.e., a highly irregular, porous support such as PVG, where the adsorbate does not uniformly distribute throughout the entire pore volume, however, surface coverage cannot be uniquely defined. Rather, only limits of surface coverage can be defined. In the lower limit, we assume that the entire pore volume is accessible to the adsorbate and a surface area of 130 m^2/g.[28,29] In the upper limit, we assume a surface area defined by the geometric dimensions of the sample, 17 cm^2. If one takes 6 Å as the molecular diameter of $W(CO)_6$(ads)[30] and 1.38 g/mL as the density of PVG,[29] impregnations of the regions adjacent to the outer geometric surface with ≤3.09×10^{-5} mol of complex correspond to surface coverages of ≤1% to greater than monolayer, respectively. Since adsorption of these gases is unaffected by the adsorbed complex, however, we assume that the actual surface coverage is substantially less than monolayer.

The adsorption isotherm of CO on PVG conforms to the Langmuir derivation,[31] and as shown in Figure 4a, the pressure dependence of its reaction rate constant parallels that of the isotherm. In contrast, the isotherms of *cis*- and *trans*-2-butene exhibit a more complex dependence on pressure; a representative plot for the cis isomer is shown in Figure 4b. For these alkenes, the isotherms exhibit a pronounced increase in the amount adsorbed in a region where the reaction rate constant becomes independent of alkene pressure.

Rapid equilibration also occurs when the samples are exposed to *n*-hexane solutions of the ligands. Although there are significant deviations at longer times, approximating the initial rate of bpy adsorption as first order, i.e., assuming an initial excess of binding sites, yields $k_{ads} = 9.4 \times 10^{-3}$ s^{-1} at 22 ± 1 °C. The lack of a dependence on the adsorbed complex suggests that adsorption, either from *n*-hexane solution or from the gas phase, is a random process in which these reacting ligands principally adsorb onto vacant PVG sites.

(27) Wrighton, M. S.; Ginley, D. S.; Schroeder, M. A.; Morse, D. L. *Pure Appl. Chem.* **1975**, *41*, 671.

(28) Elmer, T. H.; Fehlner, A. *J. Am. Ceram. Soc.* **1970**, *53*, 171.
(29) Janowski, V. F.; Heyer, W. *Z. Chem.* **1979**, *19*, 1.
(30) Schid, G.; Bose, R.; Wolz, E. *Chem. Ber.* **1975**, *108*, 26.
(31) Adamson, A. W. "Physical Chemistry of Surfaces", 3rd ed.; Wiley: New York, 1976; p 552.

Discussion

Adsorption from *n*-hexane and removal of the solvent in vacuo at room temperature lead to a uniform distribution of $W(CO)_6$(ads) on the surface, but not through the cross section of PVG. Regardless of the moles adsorbed, in these experiments, the complex penetrates 0.3–0.4 mm into PVG. Since similar penetration depths are found with a variety of metal complexes that differ from $W(CO)_6$ in both mechanism of adsorption and size, the penetration depth is taken as a measure of the deviations from surface planarity, rather than penetration into interior cavities. $W(CO)_6$(ads) is uniformly adsorbed onto the outer geometric surfaces of PVG. During photolysis, there is no spectral evidence of agglomerization, and the distribution of the photoproduct is assumed to be equivalent to that of the hexacarbonyl. Thus, the reactions examined in these experiments are limited to species on the outermost surfaces of PVG.

Adsorption neither disrupts the primary coordination sphere nor, assuming a correlation between bond strength and IR frequency, significantly weakens the W–CO bond. Photolysis of the physisorbed complex leads to CO evolution and formation of $W(CO)_5$(ads).[1] In low-temperature matrices, the pentacarbonyl has a square-pyramidal, C_{4v}, structure, and the sensitivity of the low-energy $^1A \rightarrow {}^1E$ transition to the matrix suggests that a matrix molecule or atom occupies the vacated coordination site.[23] There is also mounting evidence that the pentacarbonyl detected in what are generally considered to be noncoordinating solvents is $W(CO)_5S$, where a solvent molecule, S, occupies the vacated coordination position.[32] The EPR spectrum of $W(CO)_5$(ads) is consistent with a singlet ground state of C_{4v}, square-pyramidal structure, and its adsorption spectrum is similar to spectra of $W(CO)_5L$, where L is an O-donor ligand. Since hydroxylated silica surfaces can act as ligands,[5,6] the spectral data suggest that either chemisorbed water or a silanol group occupies the vacated coordination site, and the unusually long lifetime of $W(CO)_5$(ads) ($\geq$48 h in vacuo at room temperature) arises from coordination to the support.

The spectral changes that follow exposure of $W(CO)_5$(ads) to a ligand, L, either as a gas or in a solution of degassed *n*-hexane, indicate the formation of $W(CO)_5L$(ads) or $W(CO)_4$(bpy) when L is bpy. The observed reactions are limited to the photogenerated pentacarbonyl since the amount of product formed differs by $\leq$3% from the amount of $W(CO)_5$(ads) generated photochemically. A priori, formation of $W(CO)_5L$(ads) could occur by a gaseous ligand colliding with $W(CO)_5$(ads), but itself is not adsorbed or an adsorbed molecule. The flux of gaseous ligands onto the surface per second per square centimeter at 22 ± 1 °C and $P = 0.1$ atm is sufficient to account for the observed reactions, but it is not the only mode of reaction. The number of collisions with the surface, $P/(2\pi mkT)^{1/2}$, increases linearly with increasing pressure.[33] A reaction due solely to the flux of gaseous ligands onto the surface would, therefore, exhibit a linear dependence on pressure. As shown in Figure 4, however, an initial linear dependence is significantly diminished at higher pressures. Since equilibration of CO between the vapor and adsorbed phases is rapid and the dependence of k_{expt} on CO pressure parallels its adsorption isotherm, formation of $W(CO)_6$(ads) is attributed, in part, to a reaction between adsorbed CO and $W(CO)_5$(ads).

The dependence of k_{expt} on the pressure of *cis*- and *trans*-2-butene resembles that with CO. However, these rate constants become relatively independent of butene pressure in a region where the moles adsorbed sharply increases. Little, Klauser, and Amberg have described the rapid adsorption of various butenes onto PVG.[34] These molecules, initially physisorbed, undergo isomerization and polymerization, yielding C_6–C_{12} polymers.[34] The increase in the moles of butene adsorbed is attributed to polymerization since only a small fraction of free butene could be desorbed under vacuum. Although k_{expt} does not parallel the adsorption isotherms of *cis*- and *trans*-2-butene, the pressure dependence of k_{expt} also suggests two modes of reaction with these ligands. At low pressure, formation of $W(CO)_5L$(ads) could involve a collision between $W(CO)_5$(ads) and a gaseous ligand, while at higher pressures, where the surface coverage by the ligand increases, $W(CO)_5L$(ads) formation appears to involve a reaction between $W(CO)_5$(ads) and a mobile coadsorbed L.

The data point to two reaction modes but do not distinguish between them. Nevertheless, recognition of a reaction mode between adsorbed species accounts for some of the experimental observations. At low temperature, the first-order rate constants per mole of $W(CO)_5$(ads) differ by less than a factor 2. While this low discriminatory ability alludes to a reactive intermediate, the variation in the rate constants increases with increasing temperature. The latter would not be expected for a reaction rate controlled only by an activation barrier, since increasing the temperature increases surface diffusion and the probability of forming the transition state. Depending on the energetics of adsorption of these reactants, however, increasing temperature also changes the amount of adsorbed reactant. Since adsorption of these ligands appears to be spontaneous, exergonic processes, the larger variation in k_{expt} at higher temperature may reflect differences in the amount of adsorbed reactant. On the assumption that the reactions at 275 K and higher pressures principally involve adsorbed species, the bimolecular rate constants calculated from the first-order rate constants and the moles of ligand adsorbed are 3.89×10, 2.45×10, and 2.13×10^2 M^{-1} s^{-1} for the reaction of $W(CO)_5$(ads) with CO, *cis*-2-butene, and *trans*-2-butene, respectively. The larger value for *trans*-2-butene is somewhat surprising since its adsorption characteristics are similar to those of the cis isomer. On a support characterized by a relatively small fractal dimension, such as PVG, however, the difference in rate may reflect the structural differences in the isomers.[12]

In a recent flash-photolysis study, Lees and Adamson propose that the initially detected intermediate is a solvated complex, $W(CO)_5S$, where S represents methylcyclohexane.[31] Kinetic analysis of the data yields an estimate of the W–S bond energy of $\leq$3.9 kcal/mol. The activation parameters listed in Table I reflect, in part, the energetics of surface migration. Of the reactants examined in these experiments, the rates of adsorption and desorption suggest that CO is the least strongly adsorbed. On the assumption that CO possesses the smallest energy barrier to surface migration, its activation energy, $\leq$7 kcal/mol, is an upper limit of the $W(CO)_5$–PVG interaction energy. The latter involves an interaction between $W(CO)_5$ and either chemisorbed water or a silanol group through an O-donor atom. As such, it would be expected to be more exergonic than the interaction with methylcyclohexane, but it is not large enough to be considered, in the kinetic sense, as indicative of formal coordination of $W(CO)_5$ to the PVG surface. The latter would be expected to exhibit activation parameters similar to that found for the substitution reactions of $W(CO)_5X$ species where ΔH is $\sim$25 kcal/mol.[35] Rather, the kinetic estimate of the $W(CO)_5$–PVG interaction energy, $\leq$7.0 kcal/mol, indicates a weak interaction that stabilizes the adsorbed pentacarbonyl but is not a significant barrier to continued reactivity.

Conclusion

The reactions of $W(CO)_5$(ads) resemble solution-phase substitution reactions except that the reacting ligand replaces a PVG surface functionality occupying the vacated coordination site. The activation energies of the reactions indicate that the $W(CO)_5$–PVG interaction energy is $\leq$7 kcal/mol. Although the latter interaction most likely accounts for the unusually long lifetime of the adsorbed pentacarbonyl, it is not a significant barrier to reactivity.

(32) Lees, A. J.; Adamson, A. W. *Inorg. Chem.* **1981**, *20*, 4381.
(33) Atkins, P. W. "Physical Chemistry"; W. H. Freeman: San Francisco, CA, 1978; p 804.
(34) Little, L. H.; Klauser, H. E.; Amberg, C. H. *Can. J. Chem.* **1961**, *39*, 42.
(35) Angelici, R. J. *Organomet. Chem. Rev., Sect. A* **1968**, *3*, 173.

Acknowledgment. Support of this research by the Research Foundation of the City University of New York, the Dow Chemical Company's Tecnology Acquisition Program, and the donors of the Petroleum Research Fund, administered by the American Chemical Society, is gratefully acknowledged. H.D.G. thanks the Andrew W. Mellon Foundation for a fellowship during 1983–1984 and the Corning Glass Co. for samples of porous Vycor glass.

Registry No. $W(CO)_6$, 14040-11-0; $W(CO)_5$, 30395-19-8; bpy, 366-18-7; CO, 630-08-0; *cis*-2-butene, 590-18-1; *trans*-2-butene, 624-64-6; 1-pentene, 109-67-1.

Contribution from the Department of Chemistry,
Case Western Reserve University, Cleveland, Ohio 44106

Mechanism for Chelated Sulfate Formation from SO_2 and Bis(triphenylphosphine)platinum

S. P. MEHANDRU and ALFRED B. ANDERSON*

Received October 8, 1984

Structure and energy surface calculations using the atom superposition and electron delocalization molecular orbital theory show that the first step in the reaction between SO_2 and the dioxygen complex $(PPh_3)_2PtO_2$ is the coordination of SO_2 with one oxygen atom of the complex, followed by metal–oxygen bond breaking and reorientation, leading to a five-membered cyclic structure. This then rearranges to form the bidentate coordinated sulfate. Alternative pathways are considered and are found to be less favorable.

Introduction

Dioxygen transition-metal complexes have received considerable attention in the past several years because of their important role in biological processes and in catalysis. Several extensive reviews have appeared in the literature summing up the available information on a variety of these complexes.[1] The reactivities of the η^2-dioxygen ligand in low-oxidation-state transition-metal complexes have also been investigated in recent years,[2] particularly their reactions with carbonyl compounds,[3] carbon dioxide,[4] sulfur dioxide,[5] and olefins.[6] In most of these reactions the coordinated dioxygen behaves as a nucleophile. Ugo et al. have studied the kinetics of the addition of ketones to $(PPh_3)_2PtO_2$, forming a pseudo-ozonide.[7] They found the major pathway to be first order in complex and ketone. This mechanism was thought to involve coordination of the ketone to an axial site of the square-planar complex, followed by intramolecular nucleophilic attack on the carbonyl by dioxygen. Thus they postulated a S_N2-type transition state for this reaction. Collman et al.[5] have shown from isotopic labeling studies and IR spectroscopy that the coordinated sulfate formed by the reaction between SO_2 and the dioxygen complex of iridium gives an identical isotopic substitution pattern for the two external oxygens, irrespective of whether they start with doubly labeled O_2 or doubly labeled SO_2. They explained this result by postulating the formation of a peroxysulfite intermediate, which is analogous to the pseudo-ozonide in the case of ketones. The postulated structure of this intermediate is, however, not identical in ref 5a and 5b. In the former, one oxygen atom of SO_2 is attached to the central metal atom, forming a five-membered cyclic structure, whereas in the latter, the sulfur atom from SO_2 bonds to the metal atom, forming a four-membered ring. However, in both cases the O–O bond originating from the dioxygen ligand remains intact. It is the metal–oxygen bond that breaks in the primary step of SO_2 attack on the complex.

There has been no theoretical investigation on the mechanistic details of the steps involved in the ultimate formation of coordinated sulfate. The purpose of this paper is to calculate structures and relative stabilities for the various species possibly involved in the formation of coordinated sulfate by the reaction between SO_2 and the square-planar dioxygen complex of platinum and thus devise a reaction path for this process. We use the atom superposition and electron delocalization molecular orbital (ASED–MO) technique, which has been successfully applied to related problems, including sulfate formation mechanisms in the absence as well as in the presence of transition-metal centers,[8a-c] and to structure determinations of transition-metal coordination compounds.[8d,e] The emphasis of this work is on the molecular orbital theory of the bonding. The interaction energies calculated in this work are approximate and depend on the atomic parameter choices. Within this parameter choice, the relative interaction energies for the structures studied are expected to be in the correct order. Our orbital analyses support this expectation by explaining the bonding in terms of molecular orbital symmetry and overlap considerations, which are not qualitatively sensitive to parameter uncertainty. Theory parameters are in Table I. These parameters include ionization potentials whose spacings are based on experimental sources and therefore include the relativistic shifts that occur for platinum.

Results and Discussion

We used peroxobis(phosphine)platinum, $(PH_3)_2PtO_2$, as a simplified model for the known compound peroxobis(triphenylphosphine)platinum, $(PPh_3)_2PtO_2$, for all calculations. The O–O bond length of coordinated dioxygen was fixed at the experimental value of 1.51 Å and determined by X-ray measurements,[9] and the rest of the structure was completely optimized, with bond

(1) (a) Gubelmann, M. H.; Williams, A. F. *Struct. Bonding (Berlin)* **1983**, *55*, 1 and references cited therein. (b) Boca, R. *Coord. Chem. Rev.* **1983**, *50*, 1 and references cited therein.
(2) (a) Valentine, J. S. *Chem. Rev.* **1973**, *73*, 235. (b) Choy, V. J.; O'Connor, C. J. *Coord. Chem. Rev.* **1972/1973**, *9*, 145. (c) Tatsuno, Y.; Otsuka, S. *J. Am. Chem. Soc.* **1981**, *103*, 5832. (d) Vaska, L. *Acc. Chem. Res.* **1976**, *9*, 175. (e) Henrici-Olive, G.; Olive, S. *Angew. Chem., Int. Ed. Engl.* **1974**, *13*, 29.
(3) (a) Ugo, R.; Conti, F.; Cenini, S.; Mason, R.; Robertson, G. B. *J. Chem. Soc., Chem. Commun.* **1984**, 1498. (b) Hayward, P. J.; Blake, D. M.; Wilkinson, G.; Nyman, C. J. *J. Am. Chem. Soc.* **1970**, *92*, 5873.
(4) Hayward, P. J.; Blake, D. M.; Nyman, C. J.; Wilkinson, G. *J. Chem. Soc. D* **1969**, 987.
(5) (a) Horn, R. W.; Weissberger, E.; Collman, J. P. *Inorg. Chem.* **1970**, *9*, 2367. (b) Valentine, J.; Valentine, D., Jr.; Collman, J. P. *Inorg. Chem.* **1971**, *10*, 219.
(6) (a) Takao, K.; Wayaku, M.; Fujiwara, Y.; Imanaka, T.; Teranishi, S. *Bull. Chem. Soc. Jpn.* **1970**, *43*, 3898. (b) James, B. R.; Ochiai, E. *Can. J. Chem.* **1971**, *49*, 975. (c) Fusi, A.; Ugo, R.; Fox, F.; Pasini, A.; Cenini, S. *J. Organomet. Chem.* **1971**, *26*, 417. (d) Dudley, C. W.; Read, G.; Walker, P. J. C. *J. Chem. Soc., Dalton Trans.* **1974**, 1926. (e) Read, G.; Walker, P. J. C. *J. Chem. Soc., Dalton Trans.* **1977**, 883.
(7) Ugo, R.; Zanderighi, G. M.; Fusi, A.; Carreri, D. *J. Am. Chem. Soc.* **1980**, *102*, 3745.
(8) (a) Anderson, A. B.; Debnath, N. C. *J. Phys. Chem.* **1983**, *87*, 1938. (b) Anderson, A. B.; Hung, S. C. *J. Am. Chem. Soc.* **1983**, *105*, 7541. (c) Mehandru, S. P.; Anderson, A. B., to be submitted for publication. (d) Anderson, A. B.; Kang, D. B. *Inorg. Chem.* **1984**, *23*, 1170. (e) Anderson, A. B.; Fitzgerald, G. *Inorg. Chem.* **1981**, *20*, 3288.
(9) Cheng, P. T.; Cook, C. D.; Nyburg, S. C.; Wan, K. Y. *Can. J. Chem.* **1971**, *49*, 3772.

0020-1669/85/1324-2570$01.50/0